*Sci. J. Fac. Sci. Menoufia Univ. Vol. V (1991). 29 - 53*

# DEPENDENCE OF ANOMALOUS MAGNETORESISTANCE ON TYPE OF ORIENTATION OF THE WEAK MAGNETIC FIELD AND IRRADIATION ENERGY IN REACTOR SHIELDING MATERIALS AT 300 K

*M. S. Zaghloul, M. Younis, A. Kany and T. Zaky*

Physics Department, Faculty of Science, Al-Azhar University, Nasr City, Cairo, Egypt.

## ABSTRACT

*The longitudinal and transverse magnetoresistances (LMR and TMR) were measured of plasticized ilmenite limonite concrete sample (PLILC). The MR was measured as a function of magnetic field (B) for different rotational angles θ (θ is the angle between the direction of both weak B and current I) at 300 K. These measurements were done again after the sample was irradiated in dry channel No 36/6 of the E-RR-I reactor. The integrated fast neutron flax > I Mev is 8.3 x 10 17 n/cm2. Different types of anomalous MR were observed especially at the two opposite directions of B befor and after the sample was irradiated. Also different shapes of negative MR were found at ± Bθ. From these data it can be seen that the type of anomalous MR and the intensity of negative area of MR are strongly dependent on the type of orientation of weak B, the value of opposite angle (θ) and irradiation energy. The experimental data are illustrated and the results are discused.*

## INTRODUCTION

The negative magnetoresistance (nMR) which accompanied by different anomalous effects was observed in dilute magnetic alloys[1]. This phenomenon was interpreted on the basis of S-d exchange interaction. Non-linear field effects in magnetic system were investigated[2]. They developed the statistical mechanical theory to treat non-linear effects of static magnetic fields (B) on systems of spin

bearing particable to liquids, and configurationlly disordered (e.g. glasses) as well as rigid lattice systems.

The MR was measured in indium and $Fe_{40}Ni_{40}B_{20}$, $Fe_{30}Ni_{40}Cr_{10}B_{20}$ amorphous alloys by pulse technique in high magnetic fields[3]. The anomalous results indicated that the main contribution to electron conductivity of In was due to the carrier of the hole Fermi surface. They assumed that the low field behaviour of the nMR arising from magnetic effects which was masked by the positive MR arising from Lorents force.

The aim of this work is to study the effects of both the orientation of weak B and irradiation energy ($E_{irr}$) on the behaviour of MR of new concrete mixer. These measurements were done under low electric and magnetic fields at T=300 K.

## EXPERIMENTAL

### Sample preparation

The concrete shield under investigation had prepared from naturally occuring Egyptian ilmente (coarse aggregate) an limonite ( fine aggregate) ores mixed with portland cement and water.A plasticizer material of 1.17 gm/$m^3$ density had been added to the above mixture in order to improve both mechanical and the neutron attenuation properties. Concrete mixes were designed to flow the absolute volum method recommended by the American concrete institute (A.C.I). The plasticized ilmenite limonite concrete shield (PL.I.L.C) ingredients of 1 $m^3$ are shown in Table 1.

Table 1 : Ingredients of 1 $m^3$ of PL.I.L.C shield

| Material | | Content |
|---|---|---|
| Coarse aggregate, Kg. (ilmente ore) | 40 - 60 mm | 722 |
| | 20 - 40 mm | 482 |
| | 10 - 20 mm | 482 |
| | 5 - 10 mm | 241 |
| Fime aggregate, Kg. (Limonite ore) | | 415 |
| Cement content, Kg. | | 350 |
| Wate, lit | | 287 |
| Water cement ratio | | 0.82 |
| Plasticizer material | | 2.25 |

**Sample irradiation**

The concrete mixer was pulverized to very fine powder and shaked very well to be homogenous. Many samples were compressed by a piston into a form of discs with equal diameter (1 cm) and equal thickness (4 mm). The intensities of the samples were measured to verify that the atoms are equally distribution in every sample (d=2.92 gm / $cm^3$). Part of these samples were irradiated in the dry channel No 36/6 of the ET-RR-I reactor. The integrated fast neutron > 1 Mev is $8.3 \times 10^{17}$ $n/cm^2$. The amount of irradiation in the samples were measured outside the reactor during equal interval times ( every week) until the decay of intensity of irradiation energy ($E_{irr}$) became normal, i.e.the samples did not radiate any amount of irradiation. These measurements were performed by using a G.M. counter.

**Measurements of magnetoresistivity**

In Fig.1 terminals 1 and 2 are used for measuring the current passing the sample, while term nals 3,5 and 4,6 are used for measuring the magnetoresistivity $(\Delta\xi/\xi o)$, $\Delta\xi/\xi_0 = \xi_B - \xi_0/\xi_0$

where $\xi_B$ is the resistivity of the sample in the presence of B and $\xi_0$ is the resistivity of sample in the absence of B. All electrodes were checked to be ohimc in contact at the investigated temperature ( T = 300 K). The measurements of LMR (J// B) and TMR ( J $\perp$ B) were done under a weak electric field ( E = 0.05 KV / cm) , where the carriers do not becom hot, and at low magnetic field up to 1.5 KG to avoid the thermomagnetic effect.

## RESULTS AND DISCUSSION

The dependence of LMR and TMR on the weak B for different rotational angles $\theta$ ($\theta$ is the angle between the direction of both B and I) at T = 300 K for PL.I.L.C sample are shown in Figs.2 and 3. The general shapes of B-Mr relationships at all $\theta$ are quadratic depences on B, i.e. $\Delta\xi/\xi_0 \alpha B^2$. Where every parabolic curve is partially negative at low B and becomes positive at relatively high B. Figs.1 and 2 show different types of anomalous MR.The appearance of negative MR (nMR) at relativel high temperature means that the nMR is not only low temperature dependent as is well - known up to 50K[4, 5], but also high temperature dependent phenomenon.In our case the nMR was appeared due to the absence of symmetry axes in concrete sample.

According to these measurements, it is intersting to analyse this experimental data which can be characterized with the following fundamental features :

1 - The rate of intensity variation of nMR in LMR is foure times larger than those of TMR, but the variation rate of positive LMR is five times bigger than that observed in positive TMR during the whole scal of B at all θ.

2 - The negative depth of LMR at all θ are more deeper that at TMR, but in the TMR the negative areas have boat shapes, i.e. the negative saturation cases were appeared with different degrees. The saturation case means that the nMR is B indepent,

$$(-L\,\Delta\xi/\xi_o\,B)_\theta \# (-T\,\Delta\xi/\xi_o\,B)_\theta \quad \text{for } T = 300\ K.$$

3 - From Figs. 2 and 3 it can be seen that the anomalous behaviours of MR are observed when the direction of B was reversed at any θ. The nMR at θ = O° is larger than that at θ = 180° in Fig. 2. Also in Fig. 3 it was found that the anomalous effects of nMR at all θ except θ = 90° are nearly closed from each other in magnetic field range 0.5-0.8 KG. This shows that the value θ and the type of orientation of weak B are strongly effective on the quantitative and qualitative behaviours of MR; $(L\Delta\xi/\xi_o)B\pm\theta),(T\,\Delta\xi/\xi_o\,B\pm\theta) \#$ const for T = 300 K.

4 - It is well known that the measurements of MR as a function of ±B under low electric and magnetic field are isotropic[6]. But in our measurements the effect of $\pm B_\theta$ on MR is asymmetric. Where the degrees of stability or unstability of nMR are controlled by a certain compensating relation between the directtions of ±θ and the type of orientation of B.

The PL.I.L.C sample contains three basic copmounds, $Fe_2O_3$ (31.2%), $TiO_2$ (26.5%) and Fe O (19.1%) by weight and many traces of elements as appeared from Tefa analysis (Table.2). The atoms of these compounds have a good ability to

change theirs arrangements when exposed to the external magnetic field, due to the high magnetic moment of these elements ( the total magnetic moments ( in units $U_B$) of Fe = 6, Ti = 4 /3 and Ca = 0[7]).

From the above mentioned it was found that the different compositions of PL.I.L.C sample and the high value of magnetic moment of iron which were created a numberous asymmetry axes. This system is responsible for the appearance of different types of anomalous effects of MR.

Table. 2 : Chemical compositions of PL.I.L.C. sample of density 2.95 / $cm^3$

| No | Material | wt. % | Density | Mol. wt. |
|---|---|---|---|---|
| 1 | $Fe_2O_3$ | 31.2 | 5.24 | 159.69 |
| 2 | $TiO_2$ | 26.5 | 5.248 | 79.9 |
| 3 | FeO | 19.1 | 5.7 | 71.85 |
| 4 | CaO | 7.89 | 3.32 | 56.08 |
| 5 | $SiO_2$ | 6.4 | 2.64 | 60.08 |
| 6 | $H_2O$ | 6.29 | 1 | 1 |
| 7 | $Al_2O_3$ | 1.47 | 3.97 | 101.96 |
| 8 | Plasticizer material | 0.7 | 1.17 | |
| 9 | MgO | 0.25 | 3.58 | 40.31 |
| 10 | So3 | 0.2 | 2.29 | 80.6 |
| | Total | 100 % | 2.95 | |

**The accurate data of the analysis of X-ray diffraction of PL.I.L.C sample befor and after irradiation.**

The sample was irradiated in the dry channel No. 36/6 of the ET-RR-I reactor.The integrated fast neutron > 1 Mev is $8.3 \times 10^{-17}$ n/cm$^2$.

The X-ray diffraction patterns were automatically recorded by using a modern philips diffractometer. The general operating conditions were as following :

Copper K- alpha radiation, 38 KV, 16 mA, slits : 1° ; 0.2 mm; 1° proportional counter and scanning velocity 2°(2θ) / min.

The two diffraction patterns of PL.I.L.C samples befor and after irradiation ($B_{irr}$ and $A_{irr}$) are shown in Fig.4. It was observed that the two patterns B and A have similar behaviours at the same angles (2θ) befor and after the sample was irradiated but in different intensities. On the other hand the intensity of the peaks of pattern B is much sharper than that in pattern A at the same 2θ. From Fig.4, it can be seen that the amount of proper amorphous part does not exceed 56% of the total compositions of the sample.

From Table.3.it was found that the spectrum lines of some compounds are the same $B_{irr}$ and $A_{irr}$ at certain 2θ. This shows that at these angles 2θ,the $E_{irr}$ has no effect on these compounds and may be called resistive angle $(2\theta)_R$. Also the spectrum line of $Fe_2O_3$ at 2θ = 33.6 is 100% $B_{irr}$ and $A_{irr}$, i.e. this value is identical with the value in the identification card.This means that the $E_{irr}$ at this angle may be suffer from completely reflection by the crystalline planes of these atoms. On the other hand different similarity in the values at different 2θ may be due to that some parte of $E_{irr}$ are asymmetry scattering and the remain parte may be

reflected according to the value of 2θ. Moreover may be the $E_{irr}$ at these angles has very weak effect on the atoms. So the absorption and emission processes are isothermic. This means that the $E_{irr.}$ was emitted or absorped by the atomic planes in equal rates.

As may seen from Table 3 at definet 2θ, the intensity of spectrum lines $A_{irr}$ are many times weaker than $B_{irr}$.This indicates that the $E_{irr}$ was consumed completely to converte the crystalline states to amorphous states at these angles, so these angles may be called inversion angles $(2\theta)_I$.

Table. 3 : Intensities of resistive angle $(2\theta)_R$ and inversion angle $(2\theta°)_I$ of groups ($Fe_2O_3.H_2O$), $Fe_2O_3TiO_2$ ($FetiO_5$) and $FeTiO_3$ ($FeOTO_2$). These groups have a symbols I, II, and III respectively.

| Groups | $(2\theta)_R$ | $(I/I_o)_B$ | $(I/I_o)_A$ | $(2\theta°)_I$ | $(I/I_o)_B$ | $(I/I_o)_A$ |
|---|---|---|---|---|---|---|
| I | 33.6 | 100 | 100 | 19 | 26 | 4 |
| | 41.3 | 30 | 30 | 21.9 | 33 | 7 |
| | | | | 41.9 | 38 | 9 |
| | | | | 48.2 | 30 | 7 |
| II | 36 | 48 | 48 | 32.5 | 32 | 8 |
| | | | 30 | 48.2 | 30 | 7 |
| | 41.3 | 30 | | 60.2 | 32 | 7 |
| | | | 12 | 32.5 | 32 | 8 |
| III | 23.9 | 12 | 30 | 48.2 | 30 | 7 |
| | 41.3 | 30 | 25 | | | |
| | 64.5 | 25 | | | | |

The dependences of LMR and TMR on weak B for different θ after the sample was irradiated ($A_{irr}$) at T = 300K are shown in Figs.5 and 6. Many types of anomalous MR were observed, Which are in contrast to the behaviours shown in Figs.2 and3 befor irradiation ($B_{irr}$). So the comparison between the anomalous MR $B_{irr}$ and $A_{irr}$ can be summerized as the following.

1 - The LMR $B_{irr}$ and $A_{irr}$ are parabolic dependent on $B^2$ at all opposite angles θ, but the relative values of LMR $A_{irr}$ are many times smaller than $B_{irr}$. Also the general shapes of nMR $B_{irr}$ at all θ are more clearness than $A_{irr}$. Moreover there are irregular distributions among the MR curves at different θ $B_{irr}$ and $A_{irr}$. This means that the $E_{irr}$ is not only distroyed the lattice structures of crystalloid atoms but also strongly effective on the behaviour of MR.

$(L\Delta\xi/\xi_o B(\theta))B_{irr} \# (L\Delta\xi/\xi_o B(\theta))A_{irr}$ for T = 300 K.

2 - The nMR were found in magnetic field ranged 0.1-0.6 KG at all θ $A_{irr}$ and at B=0.1-1.6KG)$B_{irr}$. This shows that the $E_{irr}$ may be minimize the areas of MR curves due to the increasing of resistivity as a result of phase transition;

$(nL\,\Delta\xi/\xi_o B(\theta))B_{irr} >> (nL\Delta\xi/\xi_o B(\theta))A_{irr}$ for T = 300K.

3 - The anomalous behaviours of LMR at B± θ $B_{irr}$ are more clearness than $A_{irr}$. where the negative curves of MR $A_{irr}$ for different θ are nearer from each other than $B_{irr}$, due to the decreasing rates of crystalloid states. Thus the $E_{irr}$ is considered distructive force,i.e. the asymmetry directions of atoms are increasing $A_{irr}$;

$(L\Delta\xi/\xi_o B(\theta))B_{irr} \# (L\Delta\xi/\xi_o B(\theta+180°))A_{irr}$ for T = 300K

By the same manner, the above steps of comparison between the characters of

LMR $B_{irr}$ and $A_{irr}$ are repeated themself in TMR (Figs.3 and 6) but in different rates.The saturation cases of TMR at all θ were disapeard after the sample was irrdiated.This indicates that absence of independence of MR on B $A_{irr}$ is due to the random distributions of atoms of different compounds in PL.I.L.C. sample;

$$(T\,\Delta\xi/\xi_o B_{\pm\theta})B_{irr} \# \ (T\,\Delta\xi_o B_{\pm\theta})_{A_{irr}} \text{ for } T = 300 \text{ K.}$$

The effect of $E_{irr}$ on the variation of anomalous behaviours of LMR and TMR is very larg.The relative values of positive LMR (Fig.5) are smaller than TMR at all θ (Fig. 6), a contrast occur in the normal case. On the other hand the nLMR at different θ are many times larger than nTMR. The two anomalous effects on the positive and negative MR may be attributed to the non-compensating relations among the $E_{irr}$ on the type of orientation of weak B, $(E_{irr},\theta)$, $(E_{irr},B)$ and $(E_{irr}, \sigma B)$. These measurements indicate that the anomalous behaviours of MR are not only low B, θ, T, type of orientation of B[8-21] dependent, but also $E_{irr}$ dependent phenomenon;

$$(+\text{ve } L\,\Delta\xi/\xi_o\,B_{\pm\theta})_{A_{irr}} < (+\text{ve } T\Delta\xi/\xi_o\,B_{\pm\theta})A_{irr};$$

$$(-\text{ve } L\,\Delta\xi/\xi_o\,B_{\pm\theta})_{A_{irr}} > (-\text{ve } T\Delta\xi/\xi_o\,B_{\pm\theta})A_{irr};$$

$$(L\,\Delta\xi/\xi_o\,B_{\pm\theta})_{A_{irr}} \# \ (T\Delta\xi/\xi_o\,B_{\pm\theta})A_{irr};\ \#\ \text{constant for } T = 300 \text{ K.}$$

To calculate the two contributions of MR, the measured data of MR could be written in the power series of B as the following :

$$(\Delta\xi/\xi_o\,(B,\theta)_{T=300\ K} = a_0B^0 + a_1B^1 + a_2B^2 + \ldots$$

where the first order term ( $\Delta\xi/\xi_o \sim B^1$) describes the non- parabolic term of MR

and the second order term $\Delta\xi / \xi o \sim B^2$ repersents the conventional positive parabolic term of MR.

The constants $a_0$, $a_1$ and $a_2$ are dependent on the geometry of the sample ( orientation), type of the material and temperature.

The above emperical formula was fitted by the measured LMR and TMR befor and after the sample was irradiated for calcuating the two components of MR as shown in Figs. 7 - 14.

The linear terms of MR are exhibited many types of anomalous effects $B_{irr}$ and $A_{irr}$. The irregular distributions of non-parabolic terms of LMR and TMR at $\pm B_\theta$ as shown in Figs.7 and 8 are strongly dependent on the type of orientation of weak B and θ,i.e.at B = 0.1 KG (Fig.8) there are no anomalous effects, except at θ = 90°. These behaviours of linear terms of TMR are compeletly different from in LMR (Fig. 7), i.e. at B = 0.1 KG the anmalous behaviours of all components are appeared except at θ = 90° and 180°;

$| T a_1 B |_{\pm\theta}$ # cons; for B = 0.1 KG, except $\theta = 90°$

$|La_1B|_{\pm\theta} \# | T a_1 B |_{\pm\theta}$. for T = 300k

After the sample was irradiadiated, it was found that the anomalous effects of LMR and TMR (Figs.9 and 10) are in contrast to the behaviour shown in Figs.7 and 8. In Fig.9 it was noticed that the anomalous gap of $L a_1 B^1$ at θ = (45°, 225°) is larger than that at θ = (O°, 180°). Also there is no consider gap observed at θ = O° and 270°.In Fig.10 the three linear terms of TMR at θ = 45°, 90° and 225°) are

closed from each other and at low B they not exhibited any type of anomalous effects. The relative caluclated values of L $a_1B$ and T $a_1B$ along the whole scal of weak B are nearly the same, but the effect of $\pm\theta$ on $a_1B$is different,

$$|La_1B(\theta)|A_{irr} \# | La_1B(\theta+180°) A_{irr};$$

$$|Ta_1B|_{\theta = 45°.90°, 225°} \# \text{ Cons for B = 0.3 KG;}$$

$$| La_1B,Ta_1B(\pm\theta)| \quad \# La_1B,Ta_1B (\pm\theta) |_{Airr} \text{ for T = 300 K.}$$

In Figs. 11 - 14, the calculated normal positive components of LMR and TMR $B_{irr}$ and $A_{irr}$ for all $\theta$ are linear dependent on $B^2$ as will knwn.The anomalous behaviours of these terms were observed at two opposite directions of B, but in different rates in both quantitative and qualit behaviours. The intensity of asymmetry relations of parabolic components are controlled by the $E_{irr}$ , the values of $\pm\theta$ and weak B,

$$|a_2B^2|_\theta \# | a_2B^2|_{(\theta+180°)} \text{ for LMR and TMR } B_{irr}$$

and $A_{irr}$ at T=300 K.

To examin the concept of the experimental MR as a function of power series of B, which is equal is to the summation of the two calculated terms. One of them is negative, odd power of B, and the other is positive, even power, of B. so the relation between the two terms with experimental curve of MR and B at some different $\theta B_{irr}$ and $A_{irr}$ are shown in F igs. 15 - 18. From these Figs, it can be seen that the above concept of MR summation is valid and remain as it is after the sample was irradiated.The change of positions and relative values of the two components are due to the variation of $\theta$,B and the effect of $E_{irr}$ on the asymmetry

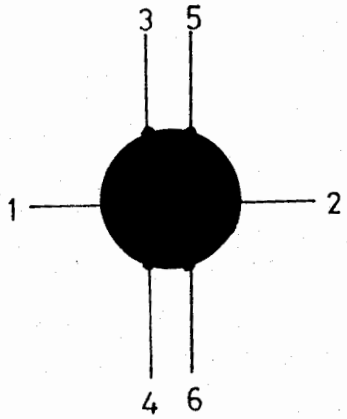


(Fig. 1) : The shape of PL.I.L.C. sample ( disc form).

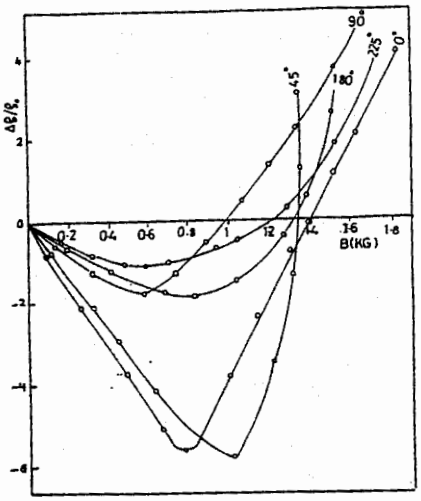


(Fig. 2) : The measured longitudinal magnetoresistivity ($L\Delta\xi/\xi_0$) as a function of magentic field (B) for different rotational angles ($\theta$) at T=300 K.

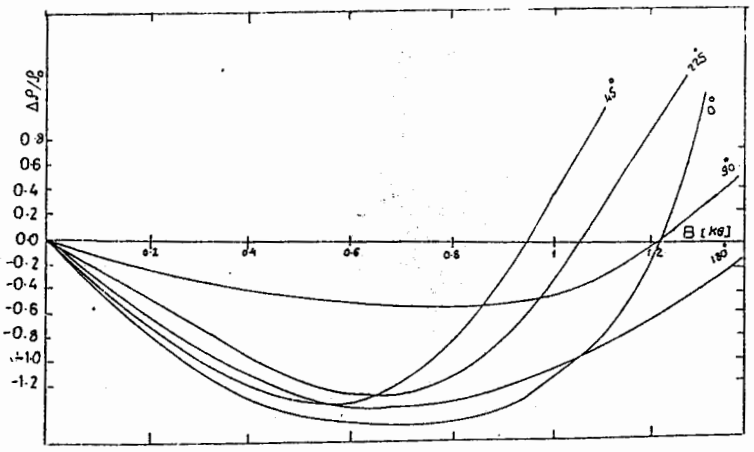


(Fig. 3) : The measured transverse Dr / ro (T $\Delta\xi$ /$\xi_O$) as a function of B for different $\theta$ at t = 300 K.

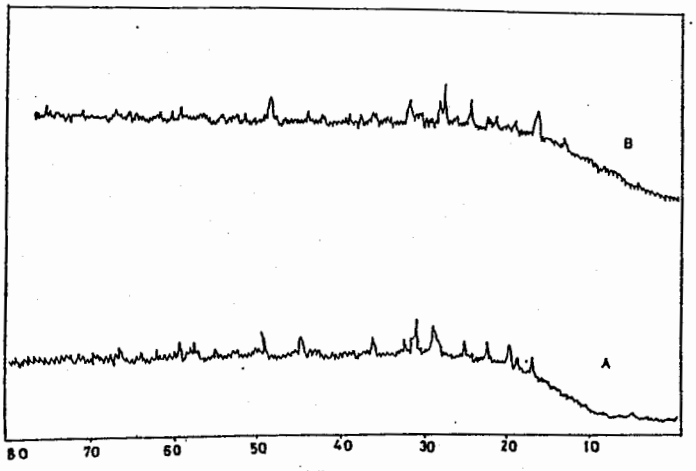


(Fig. 4) : X- ray diffraction pattern of PL.I.L.C. sample befor and after the sample was irradiated at T= 300 K.

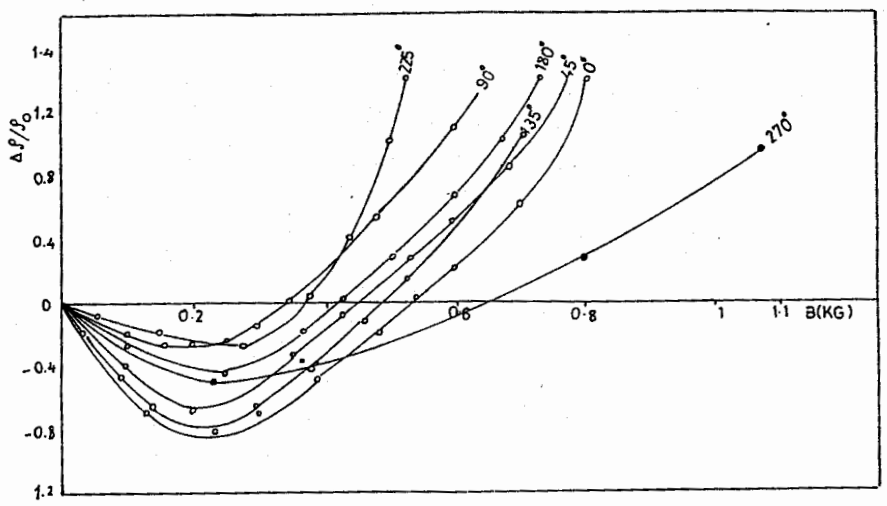


(Fig. 5) : Dependence of L $\Delta\xi / \xi_0$ on B at T = 300 K for different $\theta$, when the sample was irradiated.

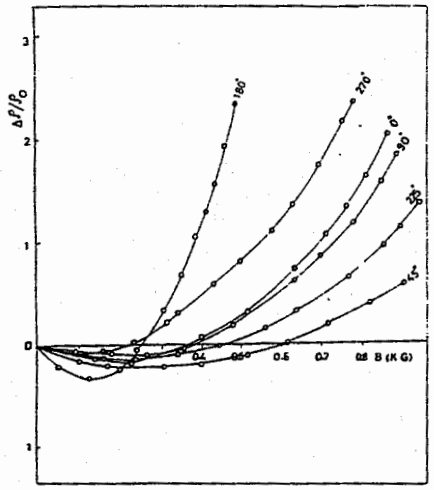


(Fig. 6) : Dependence of T $\Delta\xi / \xi_0$ on B at T = 300 K for different $\theta$, when the sample was irradiated.

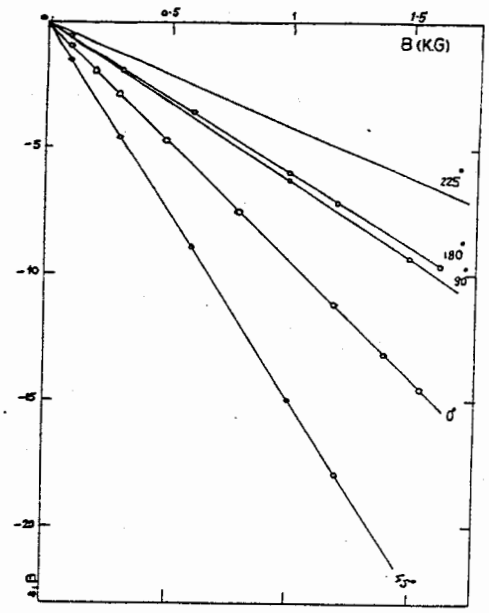


(Fig. 7) : The calulated odd components ($a_1B$) of L $\Delta\xi/\xi_O$ versus B for different $\theta$ at T = 300 K.

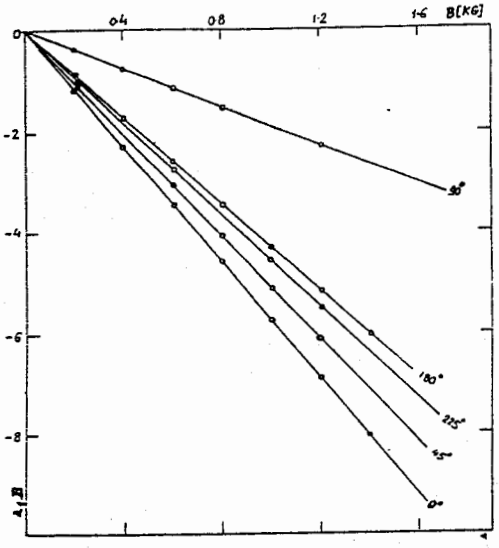


(Fig. 8) : The calculated $a_1B$ of T $\Delta\xi/\xi_O$ versus B for different $\theta$ at T = 300 K.

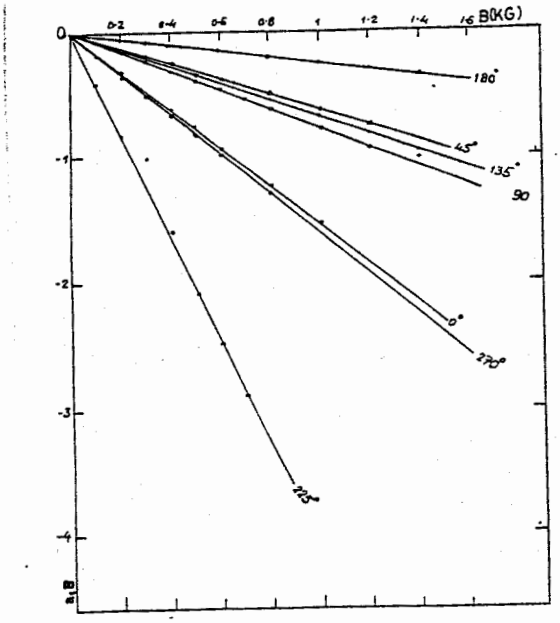


(Fig. 9) : The Calculated $a_1B$ of $L\,\Delta\xi/\xi_0$ versus B for different θ at T = 300 K, when the sample was irradiated.

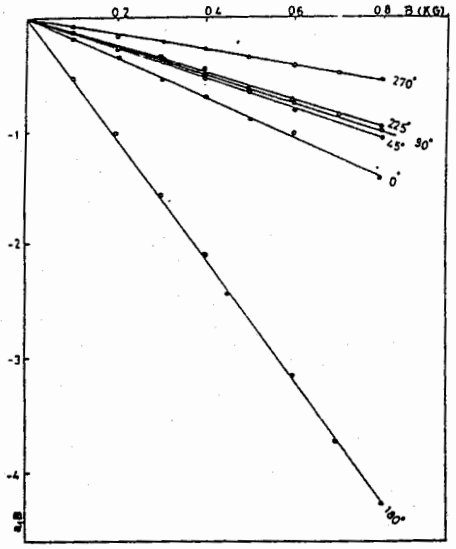


(Fig. 10) : The Calculated a1B of $T\Delta\xi/\xi_0$ versus B for different θ at T = 300 K, when the sample was irradiated.

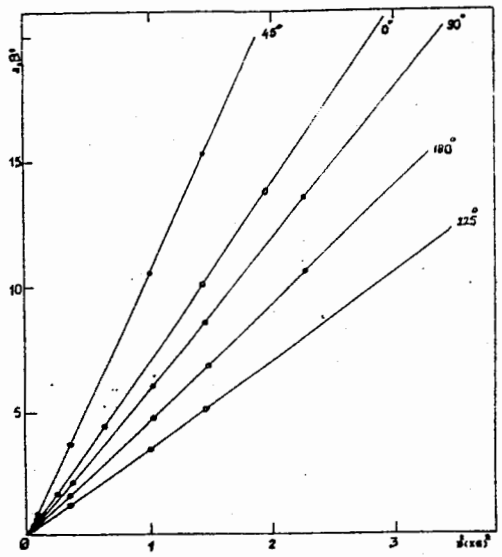


(Fig. 11) : The Calculated even components $a_2B^2$ versus B at several θ for L $\Delta\xi/\xi_0$ at T = 300 K.

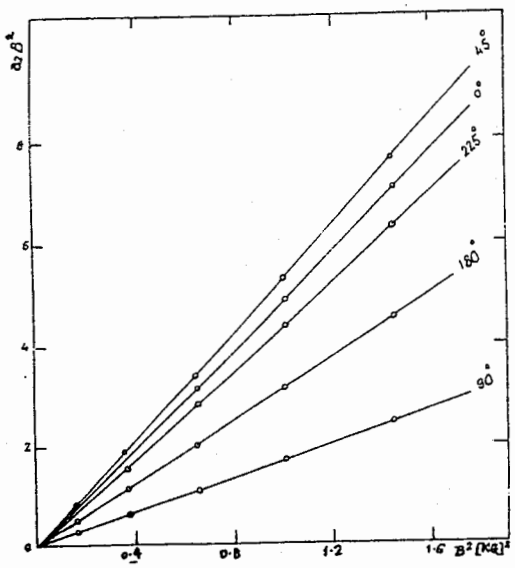


(Fig. 12) : The Calculated $a_2B^2$ versus B at several θ for T $\Delta\xi/\xi_0$ at T = 300K.

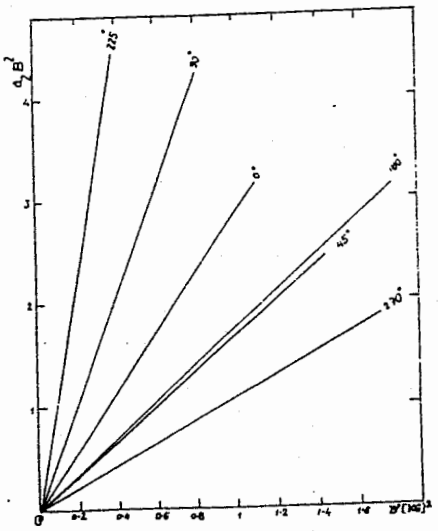

(Fig. 13) : The Calculated $a_2B^2$ versus B at several θ for $L\Delta\xi/\xi_0$ at T = 300 K, when the sample was irradiated.

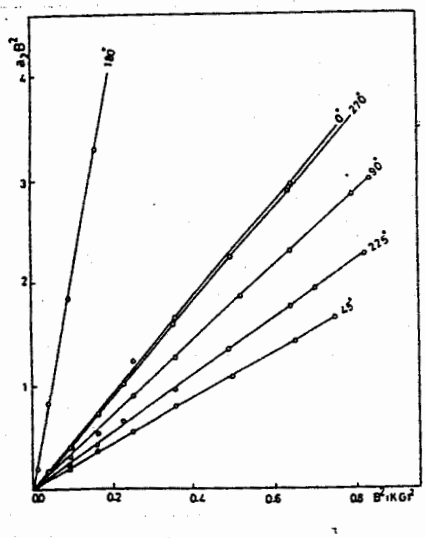

(Fig. 14) : The Calculated $a_2B^2$at several θ for $T\,\Delta\xi/\xi_0$ at T = 300 K, when the sample was irradiated.

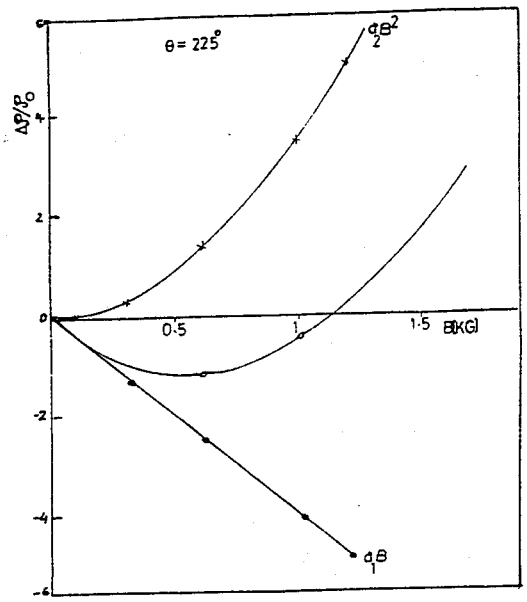


(Fig. 15) : Dependence of the measured $L\Delta\xi/\xi_0$ on B for $\theta = 225°$ at T = 300 K. The calculated anomalous $a_1B$ and normal $a_2B^2$ are represented by symbols (x) and -o-) respectively.

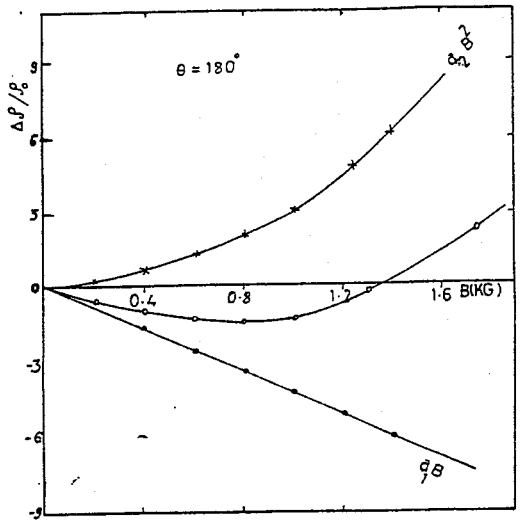


(Fig. 16) : Dependence of the measured $T\Delta\xi/\xi_0$ (-o-) on B for $\theta = 180°$ at T= 300 K. The calculated anomalous $a_1B$ and normal $a_2B^2$ are represented by symbols(-o-) and (x) respectively.

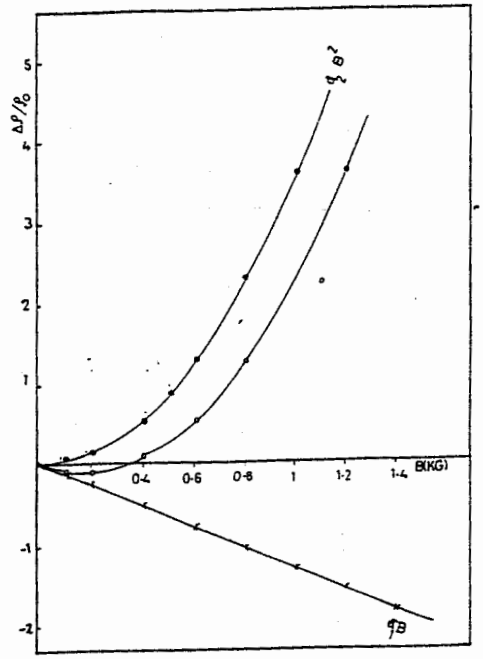


(Fig. 17) : Dependce of the measured $L\Delta\xi/\xi_0$ (-o-) on the B for $\theta = 90°$ at T = 300 K. The calculated anomalous $a_1B$ and normal $a_2B^2$ are repesented by symbols(x)and (-o-) respectively after the sample was irradiated.

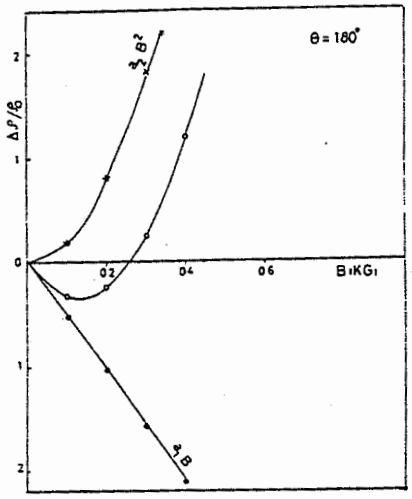


(Fig. 18) : Dependence of the measured $T\Delta\xi/\xi_0$ (-o-) on B for $\theta = 180°$ at T =300K.The calculated anomalous $a_1B$ and normal $a_2B^2$ are represented by symbols(-o-) and (x) respectively after the sample was irradiated.

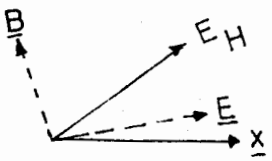


(Fig. 19) : Direction of induced Hall field ($E_H$) as a result of appliation of weak electric (E) and magnetic (B) fields, were X is the preferred direction.

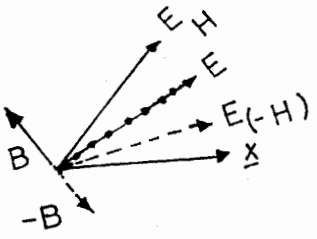


(Fig. 20) : Illustrated asymmetry relation between the induced $E_H$ at the two opposite directions of B.

axes of compounds of PL.I.L.C sample ;

$$(\Delta\xi / \xi_0 B\ (\theta)) \approx \Sigma\ \#\, La_1 B, Ta_1 B\ (\pm\theta)\ |\ _{A_{irr}} \text{ for } T = 300\ K.$$

The ratio of errors in the above expression are different according to the type of orientation and the value of $\theta$ $B_{irr}$ and $A_{irr}$. In general the errors of the above calculations were ranged from decimal fraction or hundredth.

The above results may be attributed to the absence of what is called symmetry axes in the PL.I.L.C sample. Any aggregate is characterized by a small parts have a crystalline nehaviours and may called quasi- crystals or crystalloids. This system is said to have a preferred orientation, or texture, which each grain in the polycrystalline part normaly has a crystallographic orientation, which is different from that of its neighbours. Considered as a whole, the orientations of all grains may be rondomly distributed in relation to the same selected fram of reference, or may tend to clustor, to a greater or degree about some particular orientation or orientations.

The main effect of $E_{irr}$ on the preferred orientations or texture is restrained between the distructibility of texture in different rates and vary the positions of preferred orientations. This means that befor and after the sample was irradiated there are asymmetric axes in disordered and ordered states, i.e. the direction of induced Hall field $E_H B_{irr}$ or $A_{irr}$ is not perpendicular to the directions of both electric and magnetic fields as shown in Fig.19 The absence of symmetry directions in the PL.I.L.C sample are caused in created a certain type of electric potential gradient where the intensity of this field is strongly dependent in the $\theta$ and $E_{irr}$. So according to this assumption the direction of $E_H$ at the two opposite directions of B are

asymmetrical as shown in Fig. 20.

The different types of iron oxide groups in the PL.I.L.C sample in the precence of B are induced a magnetic areas on the two sides of surfaces sample. These magnetic areas are dependent on the type of orientation of B and the intensity of interaction between the internal magnetic and external B. After the sample was irradiated the rate of induced magnetic areas are changed.All the above reasons are responsible for the variations of dynamic behaviours of different carriers such as effective mass (m*), conductivity (δ), mobility (μ) and...etc;

$$\Delta\zeta/\xi_o = \frac{\sigma(o) - \sigma(B)}{\sigma_B} = \frac{\mu(o) - \mu(B)}{\mu(B)}$$

## REFERENCES


1. G.Sadisiy, phys. Rev. 28, 131 (1962).
2. I. Steven and G. Stell, Phys. Rev B, 26, 1389(1982).
3. P. CZarnecki and M. Surma. Acta. Phy. Pol. A 64, 31 (1983).
4. K. Yasida. and H. Fukuyama, Phys. Soc. Japan, 48. 6 (1980).
5. D. K. McDonald, in Handbuch der Physik, 14, 137 (1956).
6. Y. Katayama and Tanaka, Phys. Rev, 153, 873 (1967).
7. S. V. Vansavsky, Handbook "Magnetism of Elementray particles" Mir Publishers Moscaw PP. 232 (1975).
8. M. S. Zaghloul and T. Porjesz, Acta. Phys. Hung, 48, 67 (1980).
9. M. S. Zaghloul and A. El-Sharkawy, Rev. Roum. Phys, 10, 915(1984).
10. M. S. Zaghloul and A. El-Sharkawy, Acta. Phys. Pol, A 68 59 (1985).
11. M. S. Zaghloul and A. El-shaekawy, Fiz. Yu, 16, 253 (1984):

12. M. S. Zaghloul; Fiz. Yu, 19, 51 (1987).

13. M. S. Zagloul, Indian. J. Phys, 63A, 173 (1989).

14. M. S. Zaghloul, Indian. J. Pure Applied Phys, 27, 111 (1989).

15. M. S. Zaghloul, A. Ahmed and F. Hegazy. Czech. J. Phys, B 39, 207 (1989).

16. M. S. Zaghloul and A. Ahmed, Bul. J. Phys, 16, 402 (1989).

17. M. S. Zaghloul, Bul. J. Phys, 16, 48 (1989):

18. M. S. Zaghloul, Canand. J. Phys, 67, 984 (1989).

19. M. S. Zaghloul, Physica B, Holland, 172, 392 (1991).

20. M. S. Zaghloul, Cem. Conc. Rec. U.S.A., 21, 426 (1991).

21. M. S. Zaghloul and F. Hegazy, J. Phys. Astron. Turk, Ist, 55, 151 (1991).